Applied Surface Science 334 (2015) 165–168

Contents lists available at ScienceDirect

Applied Surface Science

journal homepage: www.elsevier.com/locate/apsusc

Enhanced durability of designated polarization of $PbTiO_3$ nanodot arrays investigated by piezoresponse force microscopy

Jiyoon Kim [a], Kwang-Won Park [b], Jongin Hong [b,*], Kwangsoo No [a,*]

[a] Department of Materials Science and Engineering, KAIST, Daejeon 305-701, Republic of Korea
[b] Department of Chemistry, Chung-Ang University, Seoul 156-756, Republic of Korea

ARTICLE INFO

Article history:
Received 15 June 2014
Received in revised form 19 August 2014
Accepted 29 August 2014
Available online 6 September 2014

Keywords:
Ferroelectrics
Retention
Lead titanate
Piezoresponse force microscopy
Nanodot

ABSTRACT

We used piezoresponse force microscopy (PFM) to investigate local domain relaxation behavior of overhanging $PbTiO_3$ (PTO) nanodot arrays on platinized silicon substrates, which were prepared by using PbO vapor phase reaction sputtering on micellar monolayer films of polystyrene-*block*-poly(ethylene oxide) (PS-*b*-PEO) loaded with TiO_2 sol–gel precursor. The overhanging PTO nanodot arrays (92% at a temperature of 100 °C for 365 min) showed better ferroelectric retention than the PTO thin films (80% at the same condition). The enhanced polarization states and the absence of depolarization field due to homogeneous electric field inside the overhanging nanodot allowed for the remarkable durability of designated ferroelectric polarization.

© 2014 Elsevier B.V. All rights reserved.

1. Introduction

Next generation nonvolatile memory devices require small bit size, long-term data retention and fast operating time [1,2]. Ferroelectric films have regarded as an outstanding candidate for such devices because a small electric field can polarize ferroelectric domains corresponding to a data bit and the data sustains without the electric field [3]. While ferroelectric random access memory (FRAM) based on the ferroelectric thin films is an everlasting topic in the nonvolatile memory community, considerable recent attention has been paid to investigating probe-based ultra-high density storage technology with ferroelectric materials [4]. Although there are massive efforts to develop ferroelectric thin films as the media for nonvolatile memory devices, the ferroelectric films may not be ideal for maintaining small domain size without collapse or crosstalk, which are serious obstacles to ultra-high density data storage [5,6]. To overcome inherently this instability, discrete ferroelectric nanostructures, such that one dot contains one bit exclusive of domain merging, have been recently prepared via various techniques including block copolymer self-assembly, anodic aluminum oxide (AAO) nanotemplate and dip-pen lithography [7–10].

An important issue in applying ferroelectric nonvolatile memories and data storage devices would be a polarization relaxation phenomenon, where progressive polarization loss reduces the bit signals corresponding to the two logic states: "1" and "0" [11]. Once the polarization loss begins, it expands lateral via the reversed domain [12,13]. This reduction makes distinguishing these different logic states difficult and decreases the reading ability of stored data. Although the retention characteristics of ferroelectric materials have been studied, most have been focused on ferroelectric thin films with switching dynamics or stability corresponding to the reduction of written polarization states [13–19]. Importantly, piezoresponse force microscopy (PFM) has been adopted as a powerful tool to explore local domain structures and switching behavior of the ferroelectric films at nanoscale. For example, W.S. Ahn et al. observed the retention loss phenomena of nanodomains with a diameter of 36 nm and square domains with a size of 1 and 25 μm^2 in $PbTiO_3$ (PTO) thin films fabricated by hydrothermal epitaxy on Nb-doped $SrTiO_3$ single crystals [16]. The retention loss was explained by the instability of the curved c^+/c^- domain wall and the compressive strain energy without leakage currents. A. Morelli *et al.* investigated polarization retention loss in single crystal PTO films grown by pulsed laser deposition onto $SrRuO_3/DyScO_3$ substrates by combination of PFM and conductive atomic force microscopy (c-AFM) [17]. They revealed that the presence of leakage currents was ascribed to the significant cause of polarization reversal. Furthermore, they also reported that the presence of defects at the electrode/film interface had an influence on the polarization retention loss [18,19]. Other studies in polycrystalline films suggested that the retention loss nucleated at grain boundaries and the reversed portion expanded laterally [12–15,20].

* Corresponding authors. Tel.: +82 28205869 (J. Hong); +82 42 350 4116 (K. No).
E-mail addresses: hongj@cau.ac.kr, hong.jongin@gmail.com (J. Hong), ksno@kaist.ac.kr (K. No).

http://dx.doi.org/10.1016/j.apsusc.2014.08.171
0169-4332/© 2014 Elsevier B.V. All rights reserved.

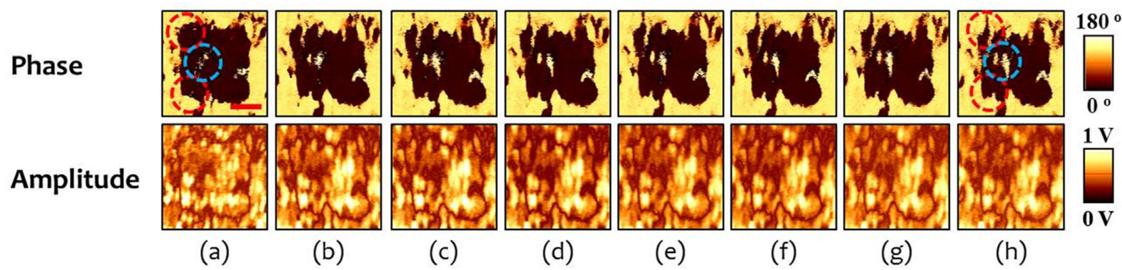

Fig. 1. Evolution of the tip-induced polarization of the box pattern in the PTO thin film over time: (a) poling, (b) 20 min, (c) 30 min, (d) 40 min, (e) 50 min, (f) 80 min, (g) 110 min and (h) 170 min. Scale bar represents 200 nm.

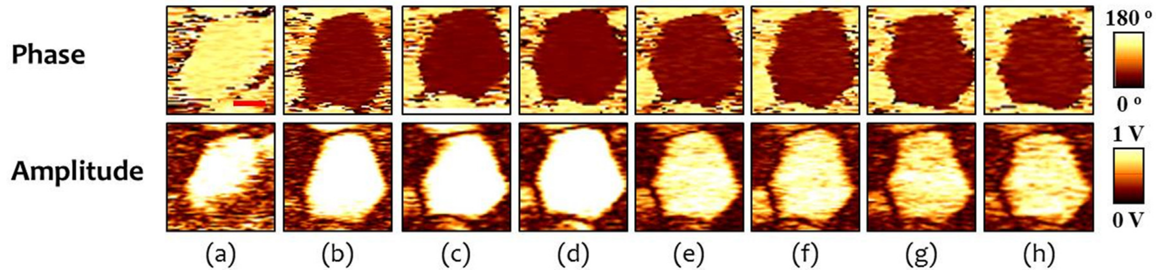

Fig. 2. Evolution of the tip-induced polarization of the PTO nanodot over time: (a) virgin, (b) poling, (c) 35 min, (d) 65 min, (e) 95 min, (f) 200 min, (g) 280 min, (h) 365 min. Scale bar represents 20 nm.

These studies, however, may not apply to domain evolution in the ferroelectric nanostructures since the electric field or polarization charge distribution of ferroelectric nanostructures is quite different from that of ferroelectric thin films. Accordingly, direct observation of ferroelectric nanostructures is crucial to determine whether they are useful for ultrahigh-density data storage with consistent stability of written domains. In this article, we firstly report the retention characteristics of ferroelectric PTO nanodots investigated by PFM.

2. Experimental procedure

Polycrystalline PTO thin films (20 nm in thickness) and PTO nanodot arrays (40 nm in height and 60 nm in diameter) were prepared on a platinized silicon substrate using PbO vapor phase reaction sputtering with TiO_2 seeds. Detailed fabrication conditions can be found in our previous works [10,21]. X-ray diffraction (XRD) analysis of the thin films and nanodot arrays confirmed the crystalline orientation of the PTO (1 0 0), (1 0 1) and (1 1 1) planes. In order to investigate retention characteristics, piezoresponse force microscopy (PFM) was used. PFM images were acquired using a commercial atomic force microscope (AFM, XE-100, Park System) equipped with a lock-in amplifier (SR830, Stanford Research Systems) [10,22]. An ac modulation voltage of 0.8 V_{rms} at 17 kHz was applied to the Pt-Ir coated AFM tip (CSC11 Ti-Pt, Micromasch) when acquiring phase and amplitude images of scanned areas. Initially, the PTO thin films were polarized from top to bottom with +5 V dc voltage at the tip over a scan area of 2 μm × 2 μm, a process is referred to as background poling. After the background poling, a small box pattern was written on the center of background poled area by applying −5 V dc to the tip over a 0.5 μm × 0.5 μm scan area. Differently, the designated PTO nanodots were polarized by nano-indentation with a pulse voltage of −8 V (same electric field used in the tip-induced poling of the thin films) and a pulse width of 1 s. Then, PFM images over a 1 μm × 1 μm scan area were obtained to examine the polarization states over time. The accelerated retention loss experiment was conducted by using a hot plate. Sample heating and PFM measurement were separated because the thermal noise from the heater made it difficult to measure *in situ* retention characteristics. The samples were heat treated at 100 °C in air and rapidly cooled down to room temperature before the measurement.

3. Results and discussion

Fig. 1 shows the evolution of the domain structure of the box pattern over time at 100 °C. Temperature accelerated testing accentuates the polarization relaxation process, enabling experimental measurements [23]. Dark and bright contrasts in the phase images correspond to domains oriented downward and upward, respectively. A 0.5 μm × 0.5 μm uniform polarized domain was created after poling and surrounded by 2 μm × 2 μm oppositely poled area, as shown in Fig. 1(a). Subsequently, the domain images were acquired at different time intervals after removing the external voltage and displayed in Fig. 1(b)–(h). We could observe a gradual decrease in the size of the written domain due to domain reversal. Reversed domains preferentially nucleated at domain boundaries, where the antiparallel orientation of the polarization encounters the edge of the box pattern. The lateral movement of the c^+ (upward

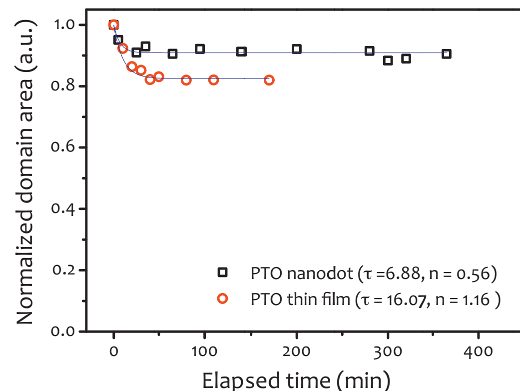

Fig. 3. Normalized domain area as a function of time. The solid lines below the normalized values denotes the exponentially fitted curves.

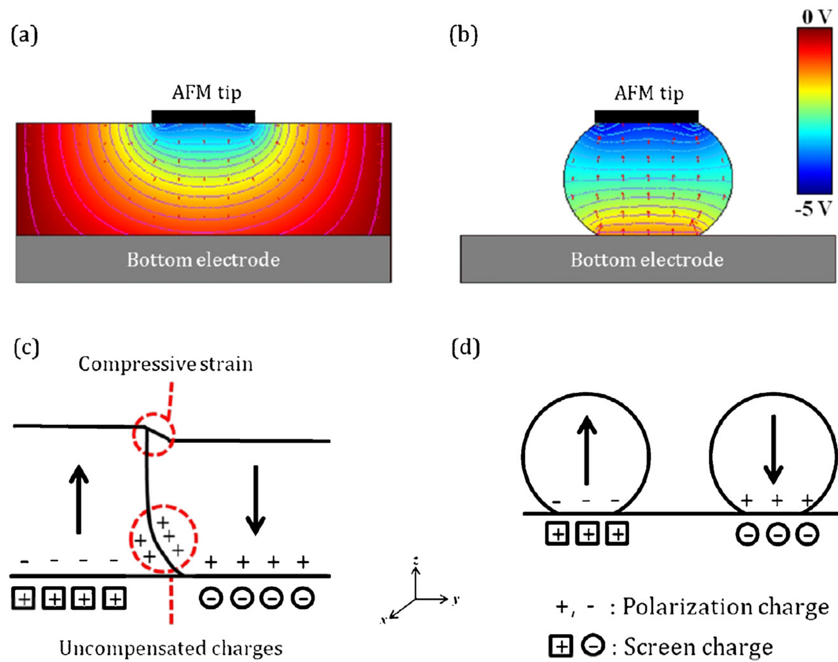

Fig. 4. Schematics of electric field lines (dashed) and equi-potential lines (solid) of (a) a PTO thin film and (b) a PTO nanodot. Schematics of polarization states of (c) box pattern in the PTO thin film and (d) dot pattern in the PTO nanodot along the thickness.

polarization)/c^- (downward polarization) domain boundary was detected in the amplitude images of Fig. 1(b)–(h). Dark contrast in the amplitude image represents such domain boundary because the amplitude reaches a minimum value when two opposite domains contribute equally to the tip vibration signal [24]. As the upward polarization reversed over time, the written area shrank and the domain boundary was curved toward its inside. The dashed circles in Fig. 1(a) and (i) indicate the domain boundaries with large curvature showing drastic domain reversal. It should be noted that, when the curvature of the domain wall is large, the domain wall moves rapidly to minimize its energy [25]. Fig. 2 shows the polarization relaxation of a PTO nanodot over time at 100 °C. Bright contrast of the virgin PTO nanodot in the phase image indicates that its initial polarization was upward polarization. The negative bias pulse flipped the polarization from top to bottom (downward polarization) and dark contrast in the phase image was obtained. The downward polarization of the PTO nanodot was attained even after 365 min, whilst the amplitude signal slightly decreased from 520 mV to 460 mV. Interestingly, unlike the retention loss of the PTO thin films, we could not observe the nucleation of any reversed domains at the resolution of our PFM.

To quantitatively analyze the dynamic behavior of retention loss, the retained domains in the polarized area at different time intervals were examined using ImageJ 1.45. Fig. 3 shows the normalized retained domains as a function of time in the PTO thin film and in the PTO nanodot. The fraction of retained domain rapidly decreased in early time and then slowly decayed. The area of the downward polarization in the PTO thin film was 80% of the initial area after 180 min, whilst the PTO nanodot retained 92% of the initial area after 365 min. A stretched exponential model was employed to investigate such polarization relaxation phenomena [12–18].

$$A(t) = C \cdot \exp\left(-\frac{t^n}{\tau}\right) + A_s \quad (1)$$

where $A(t)$ is the area fraction of retained domains correlated to time, A_s is the saturated area fraction of retained domains, C is the weighted factor of the stretched exponential, τ is the relaxation time and n is the characteristic exponent of retention loss. The fitting results obtained using Eq. (1) are denoted as solid lines in Fig. 3. The relaxation time of the PTO thin film was 16.1 min, which is comparable to that reported in the literature [13]. Interestingly, the relaxation time of the PTO nanodot was 6.9 min lower than the value of the PTO thin film. It should be noted that large τ value implies large depolarization field, which favors the immediate nucleation of reversed domains [15]. We observe that the durability of the written domains within the discrete nanodot is remarkable when compared to the polarization relaxation of ferroelectric thin films. In addition, a stretched exponent behavior with $0 < n < 1$ is characterized a dispersive transport or random walk-type process. The exponent behavior with $n > 1$ is dominated by leakage currents, which cause significant domain reversal by redistributing the charges and suppressing the electric field built in the ferroelectric layer [17].

Fig. 4 illustrates schematic diagrams of electric field lines (dashed) and equipotential lines (solid) in the PTO thin film and the PTO nanodot. Based on quantitative electrostatic calculations, the equipotential lines in the thin film are hyperbolic and the distance between each line becomes exponentially larger from the tip to the bottom electrode (Fig. 4(a)) [26]. The hyperbolic electric potential induces a curved c^+/c^- domain boundary as depicted in Fig. 4(c) [16]. In contrast, the equipotential lines in the nanodot show horizontal facets, which were induced by the uniform electric field inside of the spherical nanodot. This indicates that, when an external electric field is applied to the PTO nanodot through a conductive tip, the electric field is homogeneously distributed within the nanodot and thus the polarization charges can be completely screened (Fig. 4(d)).

In general, the domain configuration in the ferroelectric thin film depends on minimizing total free energy of the domain. The total free energy can be expressed as

$$G = G_0 + U_p + U_d + U_c + U_s + U_w \quad (2)$$

where U_p is the polarization energy, U_d is the depolarization field energy, U_c is the strain-polarization coupling energy, U_s is the strain energy and U_w is the domain wall energy. The curved c^+/c^- domain

in Fig. 4(c) results in head-to-head polarization structure and this configuration can induce depolarization field. Also, the switched c^- domain is in a compressive strain during the domain switching process and thus the strain-polarization coupling energy cannot be neglected [27,28]. However, U_s and U_w are small enough that they are paid little attention. Accordingly, the driving force of the retention loss in the ferroelectric thin film is derived from the combination of U_d and U_c. It should be noted that this is restricted to the domains in the continuous thin films. The PTO nanodots are, however, physically separated each other and thus both the depolarization field energy and the strain-polarization coupling energy cannot be induced by anti-parallel domain boundary. Moreover, the domain boundary of the PTO nanodot is shielded by its surface in the absence of adjacent anti-parallel domains. Additionally, the spherical nanodot is expected to minimize the two-dimensional clamping effect [29] and thus the strain-polarization coupling energy can be excluded from the total free energy of Eq. (2). Therefore, we think that the enhanced polarization state within the spherical PTO nanodot is attributed to the excellent durability of the written domain.

4. Conclusion

In conclusion, we investigated local polarization relaxation in the PTO thin films and nanodots. The discrete nanostructure showed an exceptional retention property when compared to the continuous thin film. The prolonged polarization state would result from the homogeneous electric field distribution inside the nanodot and less effect of substrate clamping due to its spherical shape.

Acknowledgements

This research is supported by the Basic Science Research Program (2013-026989) and Mid-career Research Program (2010-0015063, 2012-047815) through the National Research Foundation (NRF) funded by the Ministry of Science, ICT & Future Planning of Korea.

References

[1] S.Y. Wu, Ferroelectrics 11 (1976) 379.
[2] C.A. Araujo, L.D. McMillan, B.M. Melnick, J.D. Cuchiaro, J.F. Scott, Ferroelectrics 104 (1990) 241.
[3] V.R. Palkar, S.C. Purandare, R. Pinto, J. Phys. D: Appl. Phys. 32 (1999) R1.
[4] C.H. Ahn, T. Tybell, L. Antognazza, K. Char, R.H. Hannod, M.R. Beasley, O. Fisher, J.M. Triscone, Science 276 (1997) 1100.
[5] A. Hoffmann, T. Jungk, E. Soergel, Rev. Sci. Instrum. 78 (2007) 016101.
[6] N. Odagawaa, Y. Cho, Appl. Phys. Lett. 89 (2006) 192906.
[7] W. Lee, H. Han, A. Lotnyk, M.A. Schubert, S. Senz, M. Alexe, D. Hesse, S. Baik, U. Gösele, Nat. Nanotechnol. 3 (2008) 402.
[8] B.J. Rodriguez, X.S. Gao, L.F. Liu, W. Lee, I.I. Naumov, A.M. Bratkovsky, D. Hesse, M. Alexe, Nano Lett. 9 (2009) 1127.
[9] J.Y. Son, Y.H. Shin, S. Rye, H. Kim, H.M. Jan, J. Am. Chem. Soc. 131 (2009) 14676.
[10] J. Kim, J. Hong, M. Park, W. Zhe, D. Kim, Y.J. Jang, D.H. Kim, K. No, Adv. Funct. Mater. 21 (2011) 4277.
[11] A.L. Kholkin, I.K. Bdikin, V.V. Shvartsman, N.A. Pertsev, Nanotechnology 18 (2007) 095502.
[12] A. Gruveman, H. Tokumoto, A.S. Parkash, S. Aggarwal, B. Yang, M. Wutting, R. Ramesh, O. Auciello, T. Venkatesan, Appl. Phys. Lett. 71 (1997) 3492.
[13] D. Fu, K. Suzuki, K. Kato, M. Minakata, H. Suzuki, Jpn. J. Appl. Phys. 41 (2002) 6724.
[14] B.S. Sharma, S.F. Vogel, P.I. Prentky, Ferroelectrics 5 (1973) 69.
[15] V. Nagarajan, A. Aggarwal, R. Ramesh, R. Waser, Appl. Phys. Lett. 86 (2005) 262910.
[16] W.S. Ahn, W.W. Jung, S.K. Choi, Y. Cho, Appl. Phys. Lett. 88 (2006) 082902.
[17] A. Morelli, S. Venkatesan, G. Palasantzas, B.J. Kooi, J.Th.M. De Hosson, J. Appl. Phys. 102 (2007) 084103.
[18] S. Venkatesan, A. Vlooswijk, B.J. Kooi, A. Morelli, G. Palasantzas, J.Th.M. De Hosson, B. Boheda, Phys. Rev. B 78 (2008) 104112.
[19] A. Morelli, S. Venkatesan, G. Palasantzas, B.J. Kooi, J.Th.M. De Hosson, J. Appl. Phys. 105 (2009) 064106.
[20] M.Y. Park, S.B. Hong, J. Kim, Y.S. Kim, S. Buhlmann, Y.K. Kim, K. No, Appl. Phys. Lett. 94 (2009) 092901.
[21] J. Kim, S. Hong, S. Bühlmann, Y. Kim, M. Park, Y.K. Kim, K. No, J. Appl. Phys. 107 (2010) 104112.
[22] M. Park, Y.-Y. Choi, J. Kim, J. Hong, H.W. Song, T.-H. Sung, K. No, Soft Matter 8 (2012) 1064.
[23] Y. Shimada, K. Nakao, A. Inoue, M. Azuma, Y. Uemoto, E. Fujii, T. Ostuki, Appl. Phys. Lett. 71 (1997) 2358.
[24] J. Woo, S. Hong, N. Setter, H. Shin, J.-U. Jeon, Y.E. Pak, K. No, J. Vac. Sci. Technol. B 19 (2001) 818.
[25] A.J. Bray, Adv. Phys. 43 (1994) 357.
[26] A.Y. Emelyanov, Phys. Rev. B 71 (2005) 132102.
[27] W.S. Ahn, S.H. Ahn, S.K. Choi, J. Appl. Phys. 100 (2006) 114.
[28] J. Guyonnet, H. Béa, P. Paruch, J. Appl. Phys. 108 (2010) 042002.
[29] J. Kim, K.-W. Park, J. Hong, K. No, Appl. Surf. Sci. 314 (2014) 720.